

# Newton's Gravitational Constant with Uncertainty Less Than 100 ppm

M. P. Fitzgerald and T. R. Armstrong

**Abstract**— We have obtained a value for Newton's gravitational constant (coverage factor of 1) of  $G = 6.6656(6) \times 10^{-11} \text{ m}^3 \text{ kg}^{-1} \cdot \text{s}^{-2}$  with a combined standard uncertainty of 95 ppm. The method is based on a torsion balance which is servo-controlled to constant angular position with an electrostatically induced torque balancing the gravitationally induced torque. This electrostatically induced torque is calibrated using an acceleration method.

## I. INTRODUCTION

THIS paper describes a measurement of Newton's gravitational constant  $G$  using a torsion balance method. The measurement is designed to overcome many of the difficulties encountered in previous torsion balance measurements [1], [3]. The main features of this measurement are

- 1) the torsion balance is electrostatically compensated (servo-controlled to constant angular position).
- 2) the electrostatic compensation is calibrated using an acceleration method with torques much greater than those developed by the attracting masses
- 3) a reduction in the contribution to the uncertainty in  $G$  due to density variations in the suspended mass and
- 4) the measurement strategy minimizes the effects of drifts in the signal.

The design of the measurement has previously been described in some detail [4]. This paper gives a brief description of the method followed by the results of measurements and an analysis of the uncertainties in the measured value.

## II. METHOD

A schematic view of the apparatus is shown in Fig. 1. The measurement is based on a torsion balance used in a compensated mode so that the suspended mass is held at a constant angular position during the measurement. This has been shown to reduce creep in the fiber rest point [5]. Two large cylindrical masses produce a gravitationally induced torque  $\Gamma_G$  that acts on the small mass system. The small mass system is suspended from a slender fiber and consists of a cylindrical mass and a mirror. The angular position of the small mass system is measured by the autocollimator viewing the mirror. The output of the autocollimator is fed through

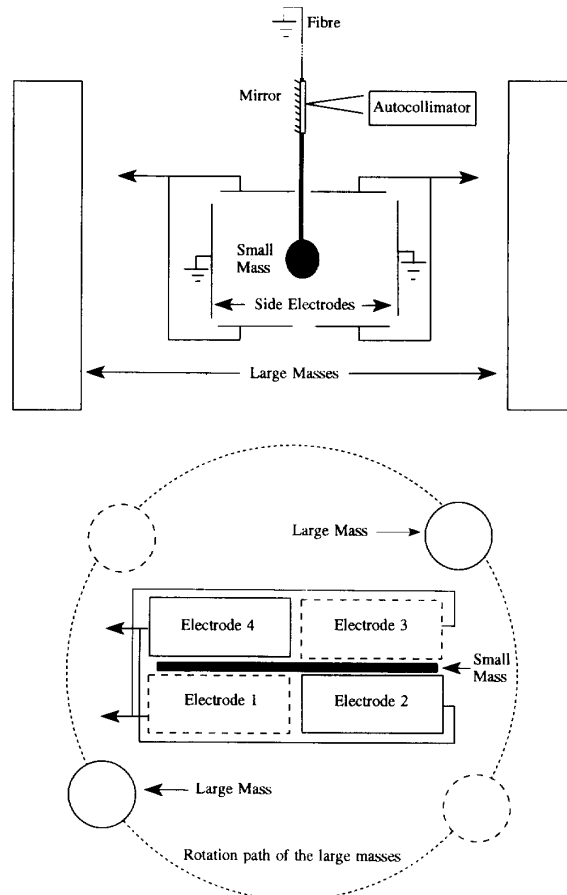


Fig. 1. A schematic representation of the torsion balance and the electrometer.

a servo-control loop to adjust the voltage  $V_G$  on each set of electrodes that surround the small mass system.

These electrodes and the small mass system constitute an electrometer. The electrostatically induced torque produced by the electrometer balances any torque acting on the small mass to maintain it at constant angular position. A novel feature of this electrometer is that the moving vane is in fact the small mass. This avoids extra electrode structures that would load the fiber and complicate the calculation of the gravitational attraction.

The torque produced by the gravitational attraction of the large masses is proportional to  $V_G^2$ . The large masses are

Manuscript received July 1, 1994; revised October 15, 1994.

The authors are with New Zealand Institute of Industrial Research, Gracefield Research Centre, Lower Hutt, New Zealand.

IEEE Log Number 9408970.

constrained to rotate about the fiber axis and values of  $V_G$  are measured at four angular positions during each revolution. These positions, shown in Fig. 1, are where  $\Gamma_G$  is at a maximum with respect to rotation angle.  $\Gamma_G$  is related to  $V_G$  by

$$\Gamma_G = 0.5 dC/d\theta V_G^2 = GK \quad (1)$$

where  $K$  is numerically calculated from the mass and geometry of the small and large masses and  $dC/d\theta$  is the change in electrometer capacitance with angular position  $\theta$  of the small mass system.

The configuration of the electrometer was chosen so that  $dC/d\theta$  is a maximum at the angular position of the small mass. This is to ensure that the restoring torque of the electrometer does not change significantly for small changes of  $\theta$ .

There are two sides to the electrometer so that torques in both clockwise and anti-clockwise directions can be produced. Consequently there are two values of  $dC/d\theta$ , one for each direction. When the masses are in the positions indicated by the solid circles in Fig. 1(b), electrodes 2 and 4 provide the restoring torque. When the masses are in the positions indicated by the dotted circles in the figure, electrodes 1 and 3 are used.

The two  $dC/d\theta$  values are determined using a variation on the acceleration method used in [6]. The large masses are removed and a constant voltage  $V_A$  is applied to one side of the electrometer. This produces a torque on the small mass system. The whole apparatus is then accelerated so that the small mass system remains at a constant angular position with respect to the electrometer. The two values are obtained from

$$dC/d\theta = 2[I\ddot{\alpha}]/V_A^2. \quad (2)$$

where  $I$  is the moment of inertia of the small mass system and  $\ddot{\alpha}$  is the angular acceleration of the apparatus.  $V_A$  is chosen to be much greater than  $V_G$  so that the torque for the acceleration is up to 300 times larger than  $\Gamma_G$ . This significantly reduces the effect of local gravitational gradients on the measurement of  $dC/d\theta$ .

By combining (1) and (2), a value of  $G$  is obtained from

$$G = V_G^2[\ddot{\alpha}/V_A^2][I/K]. \quad (3)$$

Both  $I$  and  $K$  are calculated numerically from measurements of length and mass made on the small mass system and the large masses.  $K$  is calculated from volume integration over the masses using Heyl's [7] formula for the gravitational attraction of a finite cylinder at any external point. As a check on the calculations, a point to point numerical integration over the volume of the masses has also been made.

Although both  $I$  and  $K$  depend strongly on the values of the small mass system length, density uniformity and mass, the ratio  $I/K$  does not. This is especially advantageous for the density uniformity as this is a difficult quantity to measure.

### III. EXPERIMENTAL

The small mass is constructed of copper (99.99% purity). Copper was selected as a common material with good density uniformity, low magnetic susceptibility and good electrical conductivity. The suspension fiber is a 1 m length of 0.05

mm diameter tungsten fiber. This material was chosen as it has a proven low creep characteristic [5].

The large masses are made from a single bar of austenitic 316 stainless steel which was heat treated before final finishing to minimize magnetic susceptibility. These masses are kinematically mounted on a solid aluminum turntable centered on the fiber axis. The large mass separation is a critical length measurement that is used in the calculation of the value of  $K$ . This separation of nominally 435 mm must be known to within  $\pm 2 \mu\text{m}$  so that  $K$  can be calculated with a relative uncertainty of 1 part in  $10^5$ . To achieve this a length bar comparator based on a linear variable differential transformer (LVDT) displacement transducer was developed [4]. Any density variations in the masses and the turntable are averaged by rotating the masses about their axes and shifting their mounting position with respect to the turntable.

When measuring  $V_G^2$  the large masses remain at each of the four angular positions shown in Fig. 1 for 34 minutes. This time is twice the period of any torques that may be introduced by the coupling between the horizontal and torsional pendulum modes [8] of the torsion balance. The polarity of the voltage applied to the electrometer is reversed every 17 minutes to allow the determination of the surface potentials between the stainless electrodes of the electrometer and copper of the small mass. Each average  $V_G^2$  value is corrected for the measured surface potential over each measurement period.

The apparatus is mounted on an air bearing, with a circular run out of less than  $1 \mu\text{m}$  so that it can be accurately rotated. The circular run-out at the attachment point of the fiber, about 1 m above the air bearing, is less than  $\pm 12 \mu\text{m}$ . The angular acceleration of apparatus is provided by a 25 000 step per revolution micro-stepping motor and a 360:1 worm wheel drive. Each step of the motor represents an angular step of the apparatus of  $0.8 \mu\text{rad}$ .

The angular acceleration of the apparatus is determined from measurements of the angular position of the apparatus versus time. Angular position is measured using an eight sided polygon attached to the air bearing. A second autocollimator [9] viewing the polygon is used to trigger a counter connected to a computer. The average angular acceleration is calculated by fitting a curve to the angle versus time data.

The entire measurement is computer controlled to eliminate gravitational disturbances from the movement of an operator. The angular position of the small mass system is controlled by a proportional, integral and differential (PID) control loop. The PID control loop is implemented in software to allow for the optimization of its performance in each phase of the measurement. In addition feed forward control techniques are used while shifting the large masses and starting the accelerations. This avoids large starting transients and reduces the waiting times required for the torsion balance to settle.

A typical measurement sequence lasts over 7 days. It starts by making repeat measurements of the  $\ddot{\alpha}/V_A^2$  values over a period of three days during the working week. The large masses are then positioned on the turntable and their separation measured.  $V_G^2$  values are measured over the weekend because data collected at other times is much noisier. After the weekend, the large mass separation and  $\ddot{\alpha}/V_A^2$  are remeasured.

TABLE I  
A TABLE OF THE QUANTITIES INVOLVED IN THE CALCULATION OF  $G$  WHICH HAVE A RELATIVE STANDARD UNCERTAINTY OF GREATER THAN 1 ppm IN THE FINAL VALUE OF  $G$ .  $\nu$  IN THE TABLE IS THE EFFECTIVE DEGREES OF FREEDOM IN THE VALUES.

Source of Uncertainty	Value	Standard Uncertainty		u(G) / m <sup>3</sup> ·kg <sup>-1</sup> ·s <sup>-2</sup>				Combined relative uncertainty /ppm
		Type A	Type B	Type A	ν	Type B	ν	
I/K								
Spacing /mm	435.128	0.002	0.0012	7.3x10 <sup>-16</sup>	10	4.4x10 <sup>-16</sup>	5	13
Density Uniformity /kg·m <sup>-3</sup>	7947.8		0.4			1.5x10 <sup>-15</sup>	1	22
Mass /kg	27.8949		4.2 x 10 <sup>-5</sup>			10 <sup>-16</sup>	8	1.5
Angle / rad	0.953		0.003			1.6x10 <sup>-15</sup>	1	24
Small mass height /mm	222.778		0.15			4.5x10 <sup>-16</sup>	2	7
TOTAL				7.3x10 <sup>-16</sup>	10	2.3x10 <sup>-15</sup>	2.3	36
α/V <sup>2</sup> <sub>A</sub>								
Temperature Coefficient /rad·s <sup>-2</sup> ·V <sup>-2</sup>			1x10 <sup>-13</sup>			3.0x10 <sup>-15</sup>	1	45
Polygon angles /rad	6.283185		5.4x10 <sup>-5</sup>			3.6x10 <sup>-16</sup>	10	5
Angular control / μrad	0		0.5			8.0x10 <sup>-16</sup>	25	12
Repeatability /rad·s <sup>-2</sup> ·V <sup>-2</sup>	1.12x10 <sup>-9</sup>		5.7x10 <sup>-14</sup>			3.3x10 <sup>-15</sup>	25	50
TOTAL						4.6x10 <sup>-15</sup>	5.2	68
G								
Position of large masses /rad	0.9532	0.0003		9.4x10 <sup>-17</sup>	1			1
Reproducibility /m <sup>3</sup> ·kg <sup>-1</sup> ·s <sup>-2</sup>	6.6656x10 <sup>-11</sup>	3.7x10 <sup>-15</sup>		3.7x10 <sup>-15</sup>	10			55
TOTAL				3.7x10 <sup>-15</sup>	10			55
FINAL VALUE /m <sup>3</sup> ·kg <sup>-1</sup> ·s <sup>-2</sup>	6.6656x10 <sup>-11</sup>			3.7x10 <sup>-15</sup>	11	5.1x10 <sup>-15</sup>	7.1	95

#### IV. RESULTS

The results of the measurement are discussed in terms of the quantities  $V_G^2$ ,  $\ddot{\alpha}/V_A^2$  and  $I/K$  shown in (3). Table I summarizes the quantities that contribute a relative standard uncertainty of greater than a few ppm to the result. The uncertainties have all been calculated in accordance with the ISO guide [10].

##### A. $I/K$

There are two main sources of uncertainty in  $I/K$ . These are the density non-uniformity of the large masses and the uncertainty in the angular position of the large masses with respect to the small mass system. The length comparator has enabled the combined uncertainty in the large mass spacing to be reduced to an insignificant  $2.2 \mu\text{m}$ . Kinematic mounting of the large masses has helped by allowing the masses to be replaced with a reproducibility of  $0.7 \mu\text{m}$ .

The density uniformity of the both the small and large masses was assessed by making density measurements on offcuts of the material from which they were constructed. Measurements on samples cut from the ends of the copper bar, from which the small mass was made, failed to detect differences in density at the measurement uncertainty of 3 parts in  $10^5$ . Calculations show that the ratio  $I/K$  is insensitive to density variations of this size. The large mass samples, cut in the shape of wedges and rings were taken from three different locations along the stock bar used to manufacture the large masses. The only significant variations found were radial, with

the density decreasing by 250 ppm towards the center of the cylinder. Fortunately  $K$  is largely insensitive to this kind of density variation.

##### B. $\ddot{\alpha}/V_A^2$

The electrometer calibration is typically carried out at voltages from 190–265 V. The acceleration torques produced are approximately 200–300 times the gravitational torque produced by a single field mass. Unfortunately, the apparatus is located 250 m away from a large hill which produces a gravitational gradient of around 0.1% of the accelerating torque. This gravitational gradient has been reduced by positioning masses to partially compensate for the presence of the hill. The remaining gradient is determined before each set of acceleration measurements. This is done by measuring the rest point of the torsion balance at eight different angular positions of the apparatus. The value  $\ddot{\alpha}/V_A^2$  is then corrected for this effect. The largest uncertainty in  $\ddot{\alpha}/V_A^2$  comes from the reproducibility of the results although there is a significant contribution due to the uncertainty in the temperature correction. This correction arises because the electrometer calibrations have typically been done at a temperature of up to 0.2 K higher than the measurement of  $V_G^2$ . While the electrometer has been adjusted so that  $dC/d\theta$  varies by around 10 ppm for angular movements of  $\pm 0.5 \mu\text{rad}$  it is still not exactly at its maximum. This has caused an increase in size of the temperature coefficient for  $dC/d\theta$ .  $\ddot{\alpha}/V_A^2$  has been measured throughout the six month measurement period. An analysis of

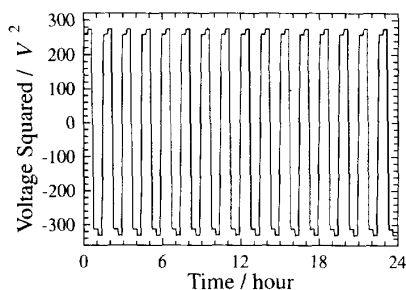


Fig. 2. Voltage squared, measured by the digital voltmeter, versus time as the large masses are shifted around the small mass system. The sign of the squared voltage indicates the direction of the induced torque.

the variances of these measurements shows that the variations between these measurement is not statistically significant. A mean value for  $\bar{\alpha}/V_A^2$  was used to calculate the value of  $G$ .

### C. $V_G^2$

A typical example of the signal obtained while measuring  $V_G^2$ , as the large masses are rotated around the small mass, is shown in Fig. 2. The sign of the squared voltage is used to indicate the direction of the applied torque. The effect of changing the electrostatic voltage polarity is clearly shown by the small steps during each 1/2 hour measurement time. As explained earlier, these steps are due to the surface potentials. We have obtained values between 0.2–0.3 V for the surface potential difference between the stainless steel of the electrometer plates and the copper of the small mass system. These potentials are stable at the milli-volt level over a twenty four hour period.

A typical Type A standard uncertainty in the mean for a  $V_G^2$  measurement over one weekend is 90 ppm.  $V_G^2$  does not appear directly in Table I because each value of  $V_G^2$  is converted to a value of  $G$  using (3). This is done because the large mass spacing can be different in each measurement due to shifting the masses to different mounting positions. The reproducibility in  $G$  is largely due to the variation in  $V_G^2$ .

The results of 10 separate determinations of  $G$  are shown in Fig. 3 plotted against the time of the measurement. The labels on the points indicate that the positions of the masses during each measurement. The labels A and B refer to the two different mounting positions with respect to the turntable while the labels 1 to 3 indicate a 120 degree rotation of each large mass about its axis. The plotted combined uncertainties are shown in the figure and are different for each measurement. This is due to variations in the size of the uncertainty in measuring  $V_G^2$ , probably caused by vibrations. An analysis of the variances shows no statistically significant differences between the results at the different large mass locations.

The overall average value obtained for  $G$  is

$$G = 6.6656(6) \times 10^{-11} \text{ m}^3 \cdot \text{kg}^{-1} \cdot \text{s}^{-2}$$

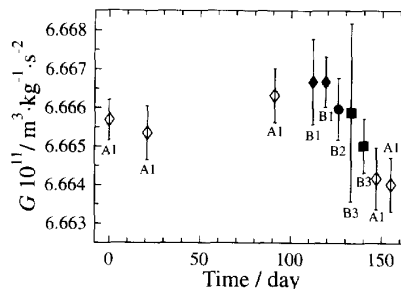


Fig. 3. The measured values of  $G$  as a function of the measurement time. The labels are described in the text.

where the 95 ppm uncertainty (14 effective degrees of freedom) is composed of a 56 ppm Type A uncertainty and a 77 ppm Type B component. This result is consistent with the most recently reported measurement of  $G$  [11].

### ACKNOWLEDGMENT

This project has involved a large number of the staff at the Measurement Standards Laboratory. In particular, we would like to acknowledge the assistance of Dr. C. Sutton for valuable discussions, P. Pickering for the length metrology, B. May for the density and mass metrology, D. Jack for his work on the electronic circuits and past and present staff of the workshop for assistance with the design and construction of the apparatus.

### REFERENCES

- [1] H. de Boer, "Experiments relating to the Newtonian gravitational constant," *Precision Measurements and Fundamental Constants II*, Nat. Bur. Stands. Spec. Publ. 617, pp. 561–572, 1984.
- [2] B. W. Petley, *The Fundamental Physical Constants and the Frontier of Measurement*. London: IOP, 1990.
- [3] G. T. Gillies and T. C. Ritter, "Torsion balances, torsion pendulums, and related devices," *Rev. Sci. Instrum.*, vol. 64, pp. 283–309, 1993.
- [4] M. P. Fitzgerald, T. R. Armstrong, R. B. Hurst, and A. C. Corney, "A method to measure newton's gravitational constant," *Metrologia*, submitted.
- [5] Y. T. Chen, A. H. Cook, and A. J. F. Metherell, "An experimental test of the inverse square law of gravitation at range of 0.1 m," *Proc. R. Soc. Lond.*, vol. A394, pp. 47–68, 1984.
- [6] R. D. Rose, H. M. Parker, A. R. Kuhlthau, and J. W. Beams, "Determination of the gravitational constant  $G$ ," *Phys. Rev. Lett.*, vol. 23, pp. 655–658, 1969.
- [7] P. R. Heyl, "A redetermination of the constant of gravitation," *J. Res. Nat. Bur. Stands.*, vol. 5, pp. 1243–1290, 1930.
- [8] P. G. Roll, R. Krotkov, and R. H. Dicke, "The equivalence of inertial and passive gravitational mass," *Ann. Phys.*, vol. 26, pp. 442–517, 1964.
- [9] T. R. Armstrong and M. P. Fitzgerald, "An autocollimator based on the laser head of a compact disc player," *Meas. Sci. Technol.*, vol. 3, pp. 1072–1076, 1992.
- [10] —, "Guide to the expression of uncertainty in measurement," Switzerland, Int. Organization for Standardization, 1993.
- [11] H. de Boer, H. Haars, and W. Michaelis, "A new experiment for the determination of the Newtonian gravitational constant," *Metrologia*, vol. 24, pp. 171–174, 1987.